

Numerical Study on Annular Tuned Liquid Dampers for Controlling the Response of Wind Towers Subjected to Seismic Loads

A.R. Ghaemmaghami & M.R. Kianoush
Department of Civil Engineering, Ryerson University, Toronto, Canada

J. Mardukhi
NCK Engineering Ltd, Toronto, Canada



SUMMARY

In this study, the performance of annular liquid tanks as tuned liquid damper (TLD) in mitigating the vibration of wind turbines due to earthquake loads was investigated using a numerical model. The structural domain was simulated using a single-degree-of-freedom (SDOF) system while the fluid domain was simulated by finite volume method (FVM). A numerical study was carried out to investigate the behaviour of annular tuned liquid damper under different earthquake records. The effectiveness of annular TLD in reducing the structural response under seismic ground motions was evaluated and discussed.

Keywords: Finite volume method, Tuned liquid damper, Passive control, Wind turbine.

1. INTRODUCTION

Wind turbines have become widespread due to a high demand for green energy all over the world. These structures are exposed to seismic hazards in high-seismic zones. The excessive structural vibration may result in the collapse of structural system under strong dynamic loads. Thus, innovative technical solutions are needed to abate the possible excessive vibration in wind turbines.

Tuned liquid dampers (TLDs) have been widely used as an efficient means to mitigate the vibration in high-rise buildings and long-span bridges, some of which are reported by Tamura et al. (1992). However, the TLDs in the shape of rectangular and cylindrical tanks which are currently used in those structures often need a large space for installation. This makes it difficult, if not impossible, for applications in the wind turbine due to an often limited space available in these structures. Alternatively, an annular TLD is proposed in this study. This ring-shaped TLD can be easily installed in a wind turbine shaft without disturbing other mechanical devices or limiting the access to the rotary system. It is expected that the use of such TLDs can lead to expand the margin of safety of these structures against earthquake loads.

The key parameters in designing a TLD are the mass ratio (defined as the ratio of the mass of the fluid to the generalized mass of the structure), the natural frequency of the liquid sloshing motion, and the inherent damping of the TLD (Fujino et al. (1988) and Sun et al. (1989)). Due to the complex dynamic behaviour of liquid-structure interaction and sloshing waves, accurate prediction of their behaviour is highly desirable.

This paper will present a numerical model to model the interaction between an annular tuned liquid damper (ATLD) and structure. The results of this study will lead to new findings on the efficiency of TLDs for the application in wind towers subjected to seismic ground motions. A large number of studies have been previously done to investigate the effect of TLDs on the dynamic behaviour of tall structures. However, most of these studies focus on the application of rectangular and cylindrical TLDs and a limited

knowledge on the behaviour of annular TLDs is available in the literature. Pioneer researches on the experimental and numerical investigation of TLDs were carried out by Fujino et al. (1988), Sun et al. (1989) and (1992) and Kareem (1990).

Reed et al. (1998) investigated the behaviour of TLD under large-amplitude excitation using experimental and numerical approaches. It was concluded that the frequency of the TLD increased as the excitation amplitude increased. Yamamoto and Kawahara (1999) developed a numerical model for simulating the behaviour of TLD. The Navier-Stokes equation was utilized in the form of the arbitrary Lagrangian-Eulerian (ALE) formulation. Tait et al. (2005) compared the results of two numerical flow models of TLD equipped with slat screens with experimental data. Jin et al. (2007) studied the effectiveness of TLDs in structural control of offshore platforms subjected to seismic ground motions using the experimental models and numerical simulation. Deng and Tait (2008) developed an equivalent mechanical model for TLDs with different tank shapes under small-amplitude seismic excitations. Later, Tait (2008) developed an equivalent linear mechanical model to calculate the amount of energy dissipated by the damping screens. In addition, Tait et al. (2008) investigated the performance of unidirectional and bidirectional TLDs under random excitation. Both efficiency and robustness of TLD were measured.

A unique study on the application of TLDs in wind turbines was carried out by Colwell and Basu (2009). They investigated the behaviour of offshore wind turbines equipped with TLCDs using a MDOF system under wind excitation. It was concluded that TLCD is efficient in reducing the structural response. It was reported that a reduction of up to 55% in the peak response of the same system can be achieved.

Tait and Deng (2010) employed an equivalent mechanical model to study structure-TLD systems and evaluate the performance of TLDs having rectangular, vertical-cylindrical or horizontal-cylindrical tank shapes, which were placed at the top of a structure. It was found that small liquid depth ratio and large mass ratio lead to a more robust structure-TLD system with small relative motion occurring between the structure and the vibration absorber. The focus of the current study is to investigate the efficiency of the proposed ATLD for the mitigation of the lateral displacement of the wind tower caused by earthquake and wind loads. As previously mentioned, there is limited research study available on the behaviour of ATLDs and in particular on the behaviour of wind turbine towers equipped with TLDs. The objective of this study is motivated by the numerical modeling of an ATLD – structure system for the application in wind turbine. A numerical model is developed to predict the dynamic interaction between fluid and structure accounting for the sloshing nonlinearity. The wind tower is modeled as a SDOF system including a rigid mass and stiffness.

2. MATHEMATICAL FORMULATION

In this study, the fluid motion is governed by Navier-Stokes equations. The equations of mass and momentum conservations of an incompressible fluid are expressed as follows in a Cartesian coordinate system:

$$\begin{aligned} \nabla \cdot (u_1, u_2, u_3) &= 0 \\ \frac{\partial(\rho u_1)}{\partial t} + \rho \nabla \cdot (u_1 u_1, u_1 u_2, u_1 u_3) &= -\frac{\partial P}{\partial x_1} + \mu \nabla^2 u_1 \\ \frac{\partial(\rho u_2)}{\partial t} + \rho \nabla \cdot (u_2 u_1, u_2 u_2, u_2 u_3) &= -\frac{\partial P}{\partial x_2} + \mu \nabla^2 u_2 \\ \frac{\partial(\rho u_3)}{\partial t} + \rho \nabla \cdot (u_3 u_1, u_3 u_2, u_3 u_3) &= -\frac{\partial P}{\partial x_3} + \mu \nabla^2 u_3 \end{aligned} \tag{2.1}$$

In which, u and p are the velocity vector and pressure over the fluid field, μ is the fluid viscosity. A multiphase flow model including water and air domains was used in this study to capture the free surface motion. The volume fractions of water and air are denoted by r_{water} and r_{air} , respectively. For example, volume fraction of water is defined by the following equation:

$$r_{Water} = \begin{cases} 0 & \text{Volume occupied by air} \\ 1 & \text{Volume occupied by water} \end{cases}$$

Based on volume fraction concept, the volume V_n occupied by fluid i in a small volume V around a point of volume fraction is given by:

$$V_i = r_i V \quad (2.3)$$

Thus, the effective density of fluid i is defined by:

$$\hat{\rho}_i = r_i \rho_i \quad (2.4)$$

3. DISCRETIZATION AND SOLUTION THEORY

In this study, the finite volume method was used to discretize the spatial domains. The fluid domain is divided into a collection of elements and nodes which are used to conserve the mass, momentum and energy. All solution variables are stored at nodes and a control volume is constructed around each node. The governing equations are integrated over each volume control and Gauss divergence theorem is applied to transform volume integrals into surface integrals. If control volumes do not change in time, the integration process can be described as follows:

$$\int_S \rho u_j dn_j = 0 \quad (3.1)$$

$$\frac{d}{dt} \int_V \rho u_i dV + \int_S \rho u_j u_i dn_j = - \int_S P dn_j + \int_S \mu \left(\frac{\partial u_i}{\partial x_j} + \frac{\partial u_j}{\partial x_i} \right) dn_j$$

Where V and S denote volume and surface regions of integration and dn_j is the differential Cartesian components of the outward normal surface vector. The next step in the numerical algorithm is to discretize the volume and surface integrals. After discretizing the volume and surface integrals using a second order backward Euler scheme, the integral equations are:

$$\begin{aligned} \sum_{NPi} (\rho u_j \Delta n_j)_{NP} &= 0 \quad (3.2) \\ V \left(\frac{(\rho u_i)_{t+1} - (\rho u_i)_{t-1}}{2\Delta t} \right) + \sum_{NPi} (\rho u_i \Delta n_j)_{NP} (u_i)_{NP} &= \sum_{NPi} (P \Delta n_i)_{NP} \\ &+ \sum_{NPi} \left(\mu \left(\frac{\partial u_i}{\partial x_j} + \frac{\partial u_j}{\partial x_i} \right) \Delta n_j \right)_{NP} \end{aligned}$$

Where, V is the volume control, Δt is the time step and Δn_j is the discrete outward surface vector. Subscript NP denotes the variable evaluated at the integration points of the control volume.

As previously mentioned, the solution variables are stored at elements nodes. In order to estimate the solution field at integration points, finite element shape function are used. According to this concept, each variable Ψ can be expressed in term of the nodal values of the variables as follows:

$$\Psi = \sum_{i=1}^N N_i \Psi_i \quad (3.3)$$

Where N_i is the shape function and Ψ_i is the value of Ψ at node i . The shape functions used in this study are linear in terms of parametric coordinates. The advective term in governing equations requires the

integration point values of any valuable Ψ to be evaluated in terms of nodal values of Ψ . The advection terms in this model can be treated in the following form:

$$\Psi_{NP} = \Psi_{up} + \beta \nabla \Psi \cdot \Delta \vec{r} \quad (3.4)$$

Where Ψ_{up} is the value at upwind node, \vec{r} is the vector from upwind node to the point NP . In this model the high resolution scheme is employed in which a special nonlinear approximation for β at each node is used. The basics of the formulation are given by Barth and Jespersen (1989).

The linear sets of equations that arise by applying the finite volume method to all elements in the domain are discrete conservative equations. Because of the trial and error nature of the linear system, a large number of iterations are typically required. The structure and fluid transfer loads across the fluid-solid interface to each other using the conservative interpolation. The staggered algorithm is based on Dirichlet-Neumann partition method which was presented by Kuttler and Wolfgang (2008) and Tukovic and Jasak (2003).

4. ERROR CONTROL AND MODEL VERIFICATION

In this study, a high-resolution scheme is employed to treat the advection terms in order to reduce the numerical error. A second order backward Euler scheme was selected as transient scheme. In addition, fine mesh spacing was used in direction of rapid solution variation to reduce the error sources. To verify the numerical model, the experimental behaviour of an annular tank which was investigated by Sun et al. (1995) is used for comparison with numerical results. The tank used in their experiments has an inside diameter of 500 mm, outside diameter of 600 mm and water height of 78 mm. The natural frequency of sloshing is equal to 0.5 Hz.

The frequency responses of wave surface elevation and the energy loss per cycle obtained from the numerical simulations and experiments are compared in Figures 4.1(a) and 4.1(b), respectively, when the amplitude of harmonic excitation is equal to 20mm. The dimensionless energy loss per cycle $\Delta E'$ is the actual energy loss per cycle, namely, the base displacement versus base shear force loop area, normalized by $m_w A^2 \omega^2 / 2$, where A is the shaking table base amplitude, ω is the excitation angular frequency, and m_w is the mass of liquid. The horizontal axes are the ratio of excitation frequency f to the first linear natural frequency f_w , of liquid sloshing in the TLD. As shown in Figure 4.1, a satisfactory agreement is seen between numerical and experimental results.

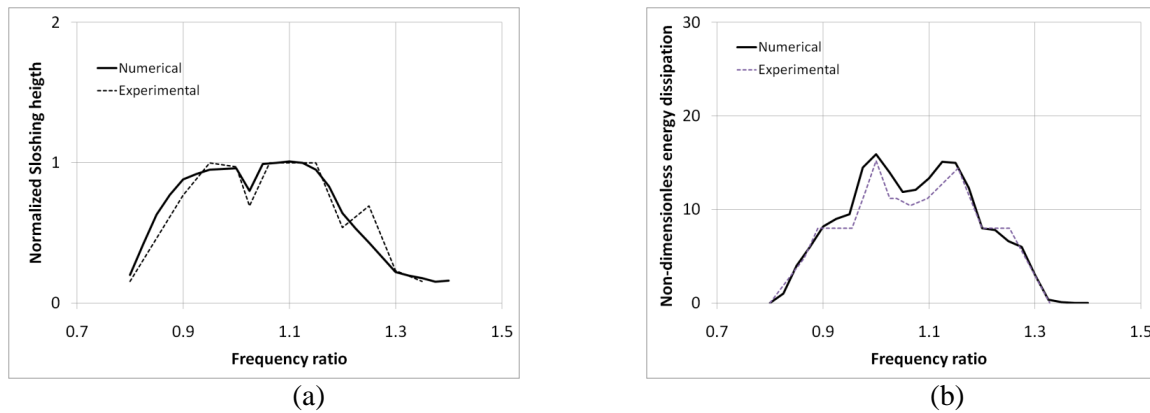


Figure 4.1: Comparison between calculated tank response using proposed numerical method and experimental results by Sun et al. (1995): (a) Non-dimensional sloshing (b) Non-dimensional energy dissipation

5. MODEL IMPLEMENTATION

As previously mentioned, the natural frequency of sloshing of the attached annular tank is tuned to the fundamental frequency of wind turbine. The height of the target wind tower is 150m which is attached to rotary system with the weight of 800 tons. Based on the proposed geometry, a fundamental frequency of 0.206Hz was derived for the wind tower using finite element analysis. The natural frequency of sloshing for an annular tank is given by the following equation:

$$\omega_n^2 = \frac{g}{R} \xi_n \tanh(\xi_n h / R) \quad (5.1)$$

Where h is the height of fluid and R the exterior radius of the tank. The values of ξ_n is given by Bauer (1960) for different ratios of interior to exterior radius (r/R). On this basis, the variation of sloshing frequency with the ratio of r/R for different water heights and $R=2.50m$ is calculated and shown in Figure 5.1.

The following dimensions are selected for annular tank in order to obtain the highest fluid to structure mass ratio and to provide sufficient space for access through the tank:

- Water height: 0.7m
- Interior diameter: 3.02m
- Exterior diameter: 5.0m

As previously mentioned, one of the key parameters in designing TLDs is the intrinsic damping of the tank. Water tank without any additional devices for suppressing the sloshing does not provide enough damping required for the optimum design of TLD. A typical ring baffle configuration consists of two rigid ring annular rings fitted around the exterior wall is chosen in this study to increase the intrinsic damping of the ATLD.

A very fine mesh grid as shown in Figure 5.1 was initially selected to carry out the numerical analyses. The time step interval was chosen as 0.005s. In this study, the wind tower is modeled as a SDOF structural system including a spring-mass system as shown in Figure 5.1. The fundamental frequency of the SDOF structural system is set to 0.206Hz which is corresponding to the in-plane bending mode of the wind tower. The system is then coupled to annular TLD tank in order to simulate the lateral response of wind tower under harmonic and random excitations.

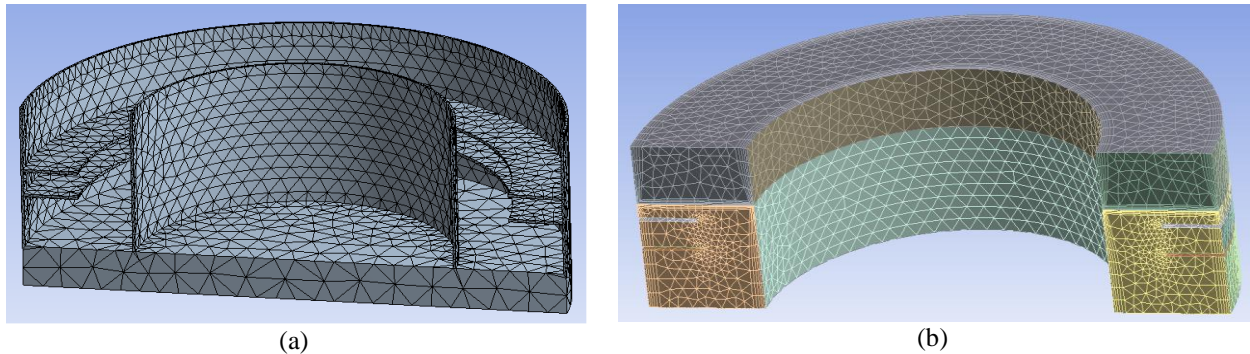


Figure 5.1: Finite element mesh: (a) Rigid tank and structural mass (b) Fluid domain

The damping ratio of the structure without the TLD is equal to 5%. The structural stiffness was equal to the product of the mass of structure and the square of the natural frequency ($k = m_s \omega_n^2$). The free ends of

springs are fixed. The rigid mass is subjected to dynamic loads in terms of time-history of ground displacement.

6. ANALYSIS RESULTS AND DISCUSSIONS

This section reports on the effect of additional effective damping, ξ_{eff} , provided to the structure using the ATLD. The objective of this study is to investigate the damping properties of an annular TLD attached to a wind tower subject to dynamic loading.

6.1 Responses to Earthquake Load

This section reports on the efficiency of ATLD in reducing the structural response of the structure subjected to earthquake records. Three different records including 1940 Imperial valley, 1995 Kobe and 1994 Northridge are chosen for the analysis purpose. The time-history of ground displacement is shown in Figure 6.1 for all records. The mass ratio of the water to the structure is assumed as 5 percent for all cases. The time-history structural response in terms of displacement has been calculated for all cases under different ground motions and is shown in Figure 6.2. It is found that the maximum calculated displacement has decreased by 23, 19 and 18 percent when the model with ring baffles is subjected to El-Centro, Kobe and Northridge earthquake records.

It can be found that the annular TLD is more efficient when the excitation amplitude is small. However, the effect of TLD on the response of the structure is dependent on the characteristics of the applied excitation.

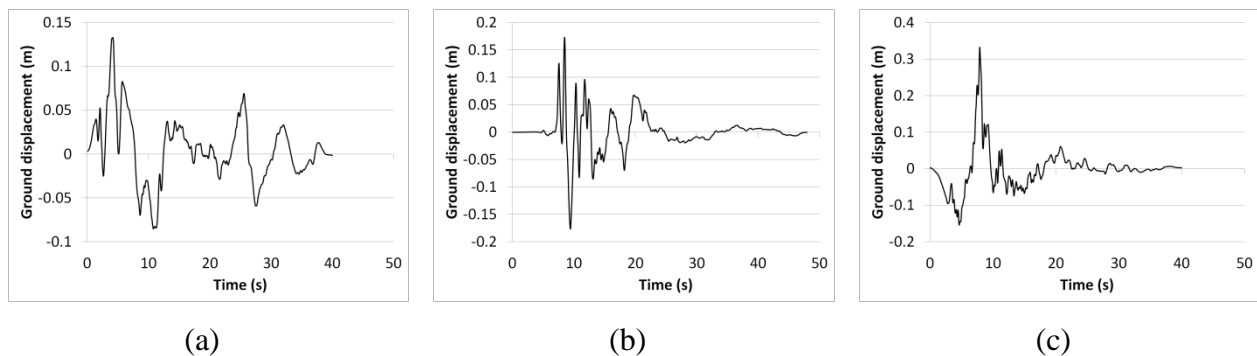


Figure 6.1: Time-history of ground motion: (a) 1940 Imperial valley (b) 1995 Kobe (c) 1994 Northridge

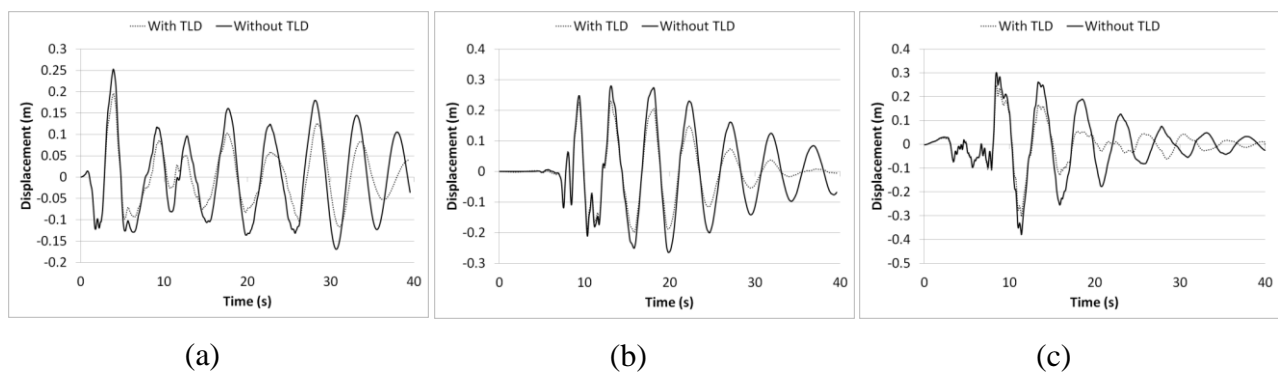


Figure 6.2: Time-history of structural displacement: (a) 1940 Imperial valley (b) 1995 Kobe (c) 1994 Northridge

7. CONCLUSIONS

A combined finite element – finite volume model was developed to account for the nonlinear behaviour of fluid sloshing and dynamic fluid-structure interaction. The accuracy and robustness of the proposed model was verified by comparing the numerical results with experimental results which are available in literature. A numerical model with TLD mass being 5 percent of the structural mass were investigated under three different seismic excitations. Numerical analyses using the proposed model were carried out to examine the performance of structure-annular TLD system. Time-history analyses were carried out in order to simulate the behaviour of ATLD-structure system under dynamic forces. Three different earthquake records including El-Centro, Northridge and Kobe were selected for the purpose of analysis. The ATLD is found effective when the system is subjected to earthquake loading. It was shown that the maximum displacement of the system could be decreased by 23 percent under selected earthquake loads.

REFERENCES

- Barth T.J. and Jespersen, D.C. (1989). "The design and application of upwind schemes on unstructured meshes", Proceedings of the 27th Aerospace Sciences Meeting, **33**, 1-12.
- Bauer H. F. (1960) "Theory of fluid oscillations in a circular cylindrical ring tank partially filled with liquid", NASA TN-D-557.
- Colwell, S. and Base, B. (2009). "Tuned liquid column dampers in offshore wind turbines for structural control". *Engineering Structures*, **31**, 358-368
- Deng, X. and Tait, M.J. (2008). "Equivalent Mechanical Models of Tuned Liquid Dampers with Different Tank Geometries", *Canadian Journal of Civil Engineering*, **35**, 1088-1101.
- Jin, Q., Li, X., Sun, N., Zhou, J. and Guan, J. (2007). "Experimental and Numerical Study on Tuned Liquid Dampers for Controlling Earthquake Response of Jacket Offshore Platform", *Marine Structures*, **20**, 238-254.
- Reed, D., Yu, J., Yeh, H. and Gardarsson, S. (1998). "Investigation of Tuned Liquid Dampers under Large Amplitude Excitation", **124(4)**, 404-413.
- Sun, L.M., Fujino, Y., Pacheco, B.M. and Isobe, M. (1989). "Nonlinear Waves and Dynamic Pressures in Rectangular Tuned Liquid Damper (TLD), Simulation and Experimental Verification", *Structural Engineering / Earthquake Engineering*, **6(2)**, 251-262.
- Sun, L.M., Fujino, Y., Chaiseri, P. and Pacheco. (1995). "The Properties of Tuned Liquid Dampers using a TMD Analogy", *Earthquake Engineering and Structural Dynamics*, **24**, 967-976.
- Tait, M.J., El Damatty, A.A., Isyumov, N. and Siddique, M.R. (2005). "Numerical Flow Models to Simulate Tuned Liquid Dampers (TLD) with Slat Screens", *Journal of Fluid and Structures*, **20**, 1007-1023.
- Tait, M.J. (2008). "Modelling and Preliminary Design of a Structure-TLD System", *Engineering Structures*, **30**, 2644-2655.
- Tait, M.J., Isyumov, N. and El Damatty, A.A. (2008). "Performance of Tuned Liquid Dampers", *Journal of Engineering Mechanics*, **134(5)**, 417- 427.
- Tait, M.J. and Deng, X. (2010). "The Performance of Structure-Tuned Liquid Damper Systems with Different Tank Geometries", *Structural Control and Health Monitoring*, **17**, 254-277.
- Tamura, Y., Kousaka, R. and Modi, V.J. (1992). "Practical Application of Nutation Damper for Suppressing Wind-Induced Vibrations of Airport Towers", *Journal of Wind Engineering and Industrial Aerodynamics*, **41(4)**, 1919-1930.
- Yamamoto, K. and Kawahara, M. (1999). "Structural Oscillation Control using Tuned Liquid Damper", *Computers and Structures*, **71**, 435-446.